Electronic Supplementary Material (ESI) for Inorganic Chemistry Frontiers.

Supporting Information File

Investigation of role of the terminal ligands on magnetic relaxation in a series of dinuclear dysprosium complexes

Siba Prasad Bera, Arpan Mondal, Sanjit Konar*

Department of Chemistry, Indian Institute of Science Education and Research Bhopal, Bhopal Bypass Road, Bhauri, Bhopal 462 066, India. E-mail: skonar@iiserb.ac.in; Fax: +91-755-6692392; Tel: +91-755-26691313.

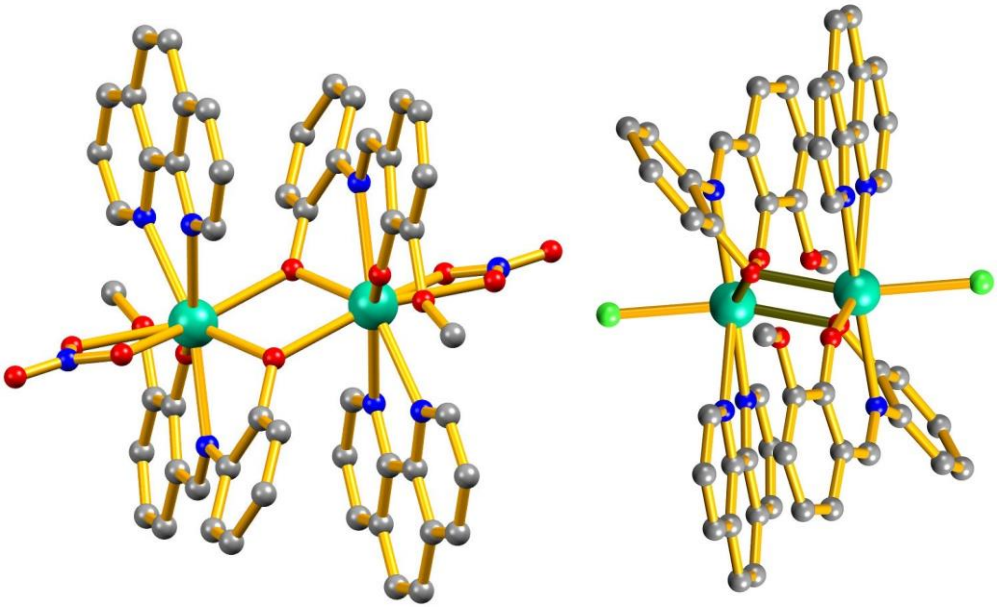

Figure S1. View of complex **2** and **3** (left and right) and hydrogen atoms are omitted for clarity {cyan, Dy; pink, P; gray, C; red, O; blue, N and green, Cl}.

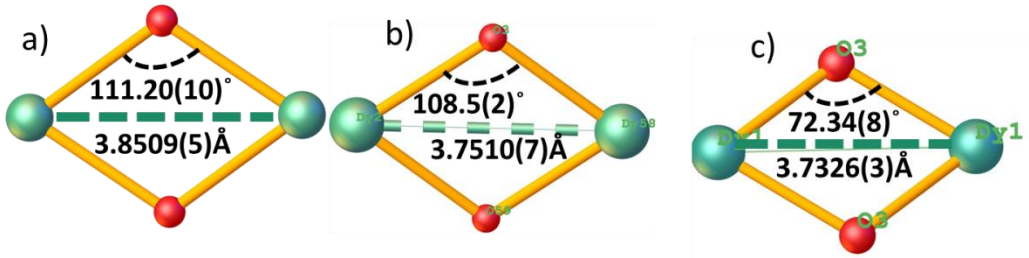

Figure S2. $Dy^{3+} \cdots Dy^{3+}$ distance and phenoxide oxygen bridging bond angle of complexes **1**(a), **2**(b) and **3**(c).

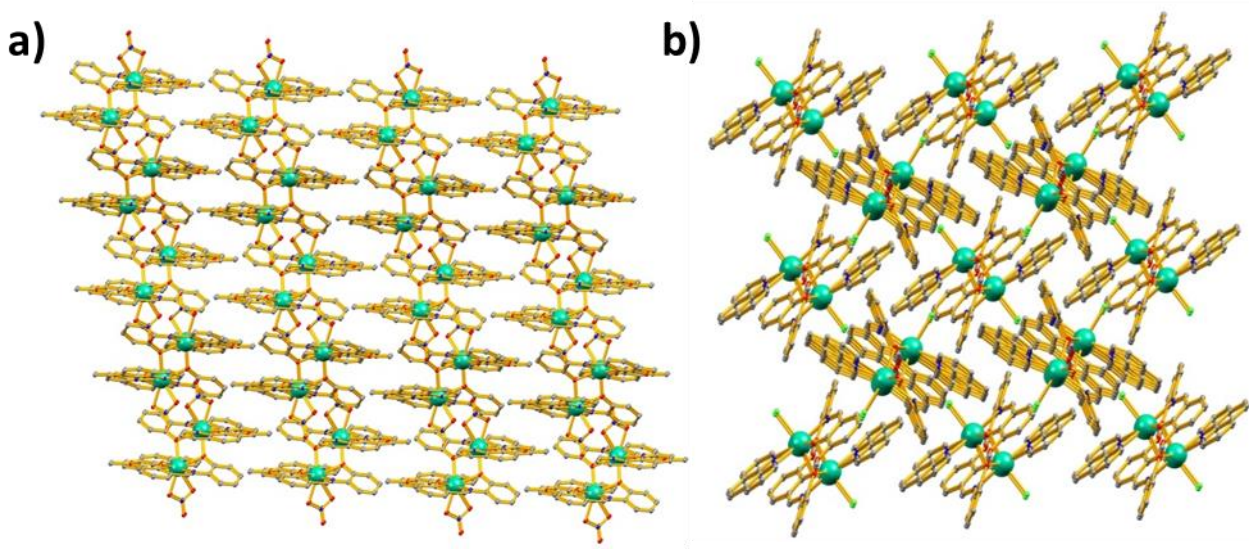

Figure S3. Packing view and shortest intermolecular $Dy^{3+}\ldots Dy^{3+}$ distance of complexes **2** (a) and **3** (b)

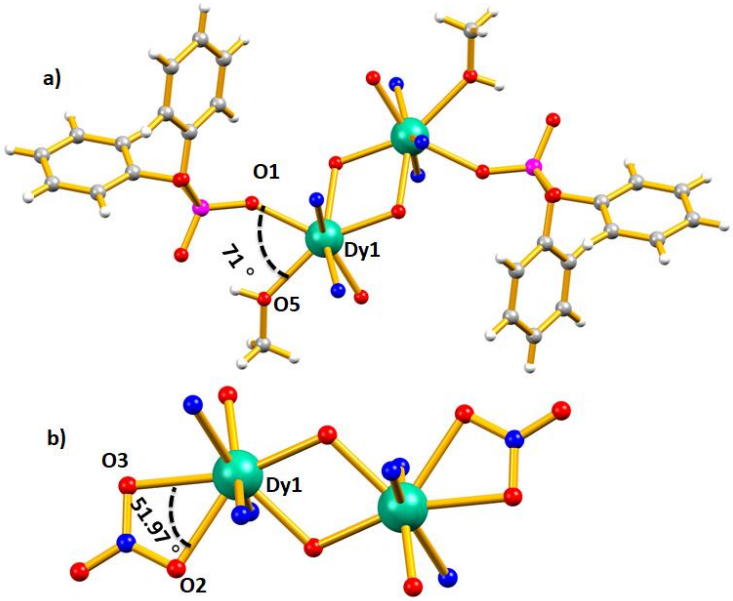

Figure S4. Bond angle of terminal oxygen with Dy^{3+} for complex **1**(a)and **2**(b).

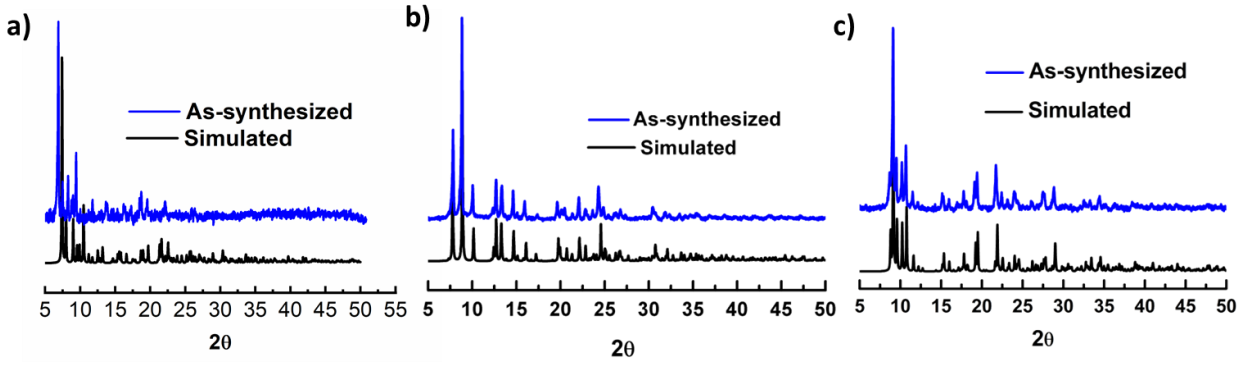

Figure S5. PXRD pattern of complexes: (a), complex **1**; (b), complex **2** and (c), complex **3**.

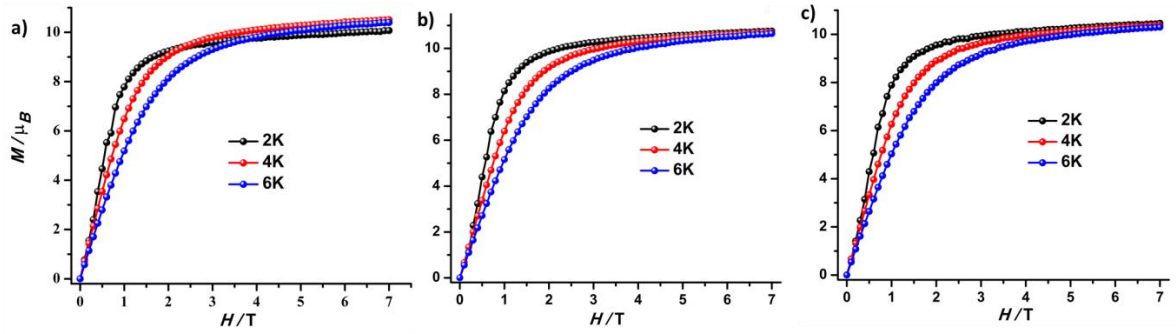

Figure S6. Field dependence of magnetization at depicted temperatures for complexes **1** (a)**, 2**(b) and **3**(c).

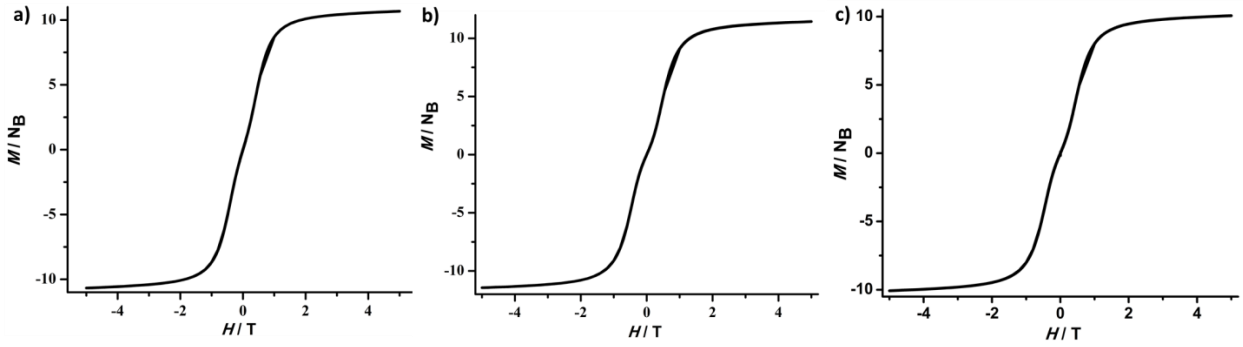

Figure S7. Hysteresis plot of complexes **1–3** (a-c) with the sweep rate 400 Oe/sec at 1.8 K.

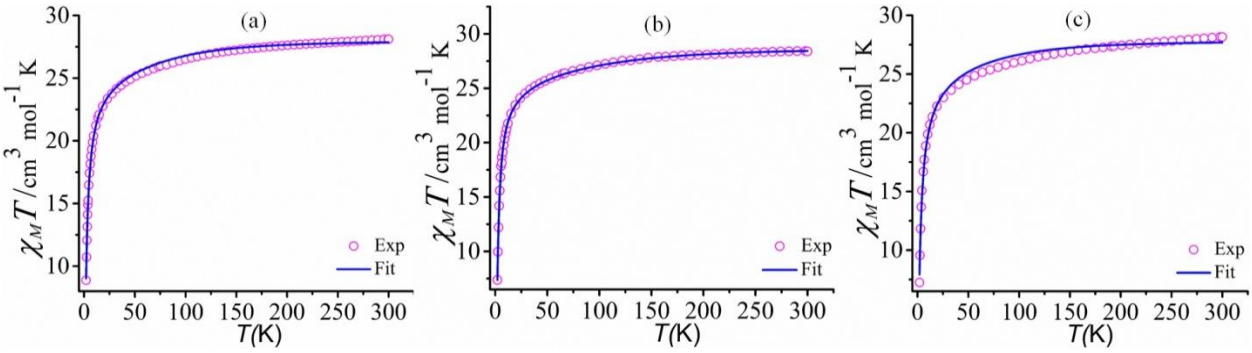

Figure S8. Experimental and simulation of χ_MT *vs* T plots using PHI software for complexes **1-3**.

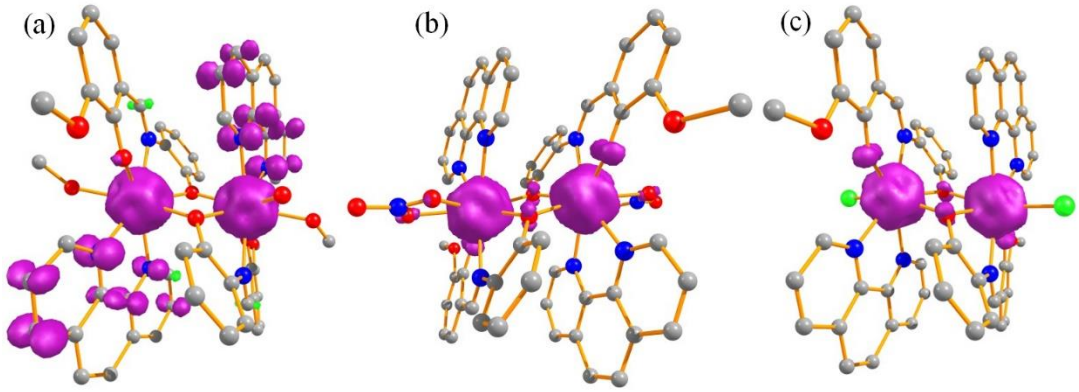

Figure S9. The spin density plots for complexes **1-3** (a-b).

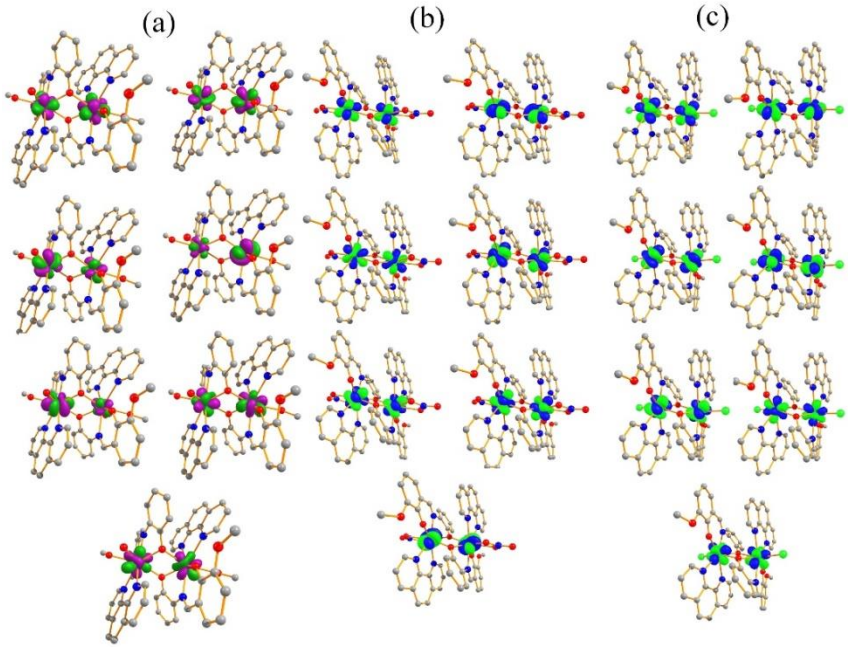

Figure S10. Magnetic orbitals of complexes **1-3** (a-c).

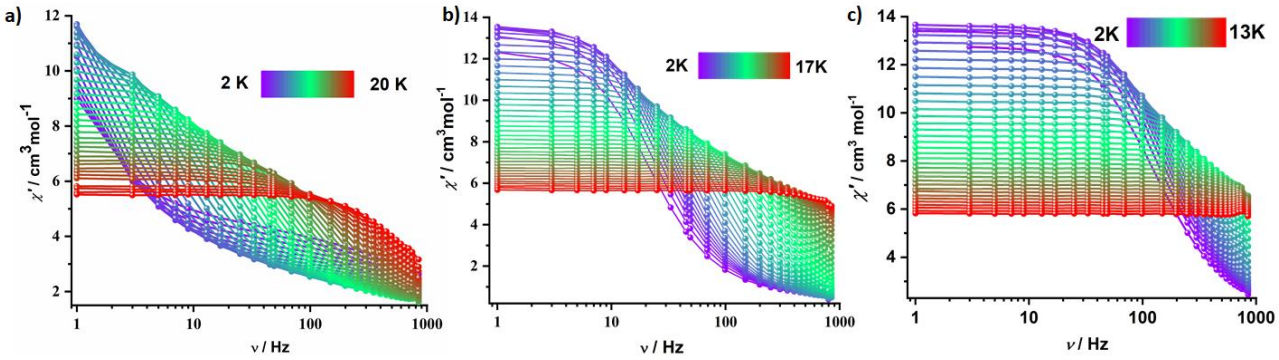

Figure S10. The out-of-phase (χ'') signals of the frequency dependence of ac susceptibility signals at given temperature in absence of DC field for complex **1-3**(a–c).

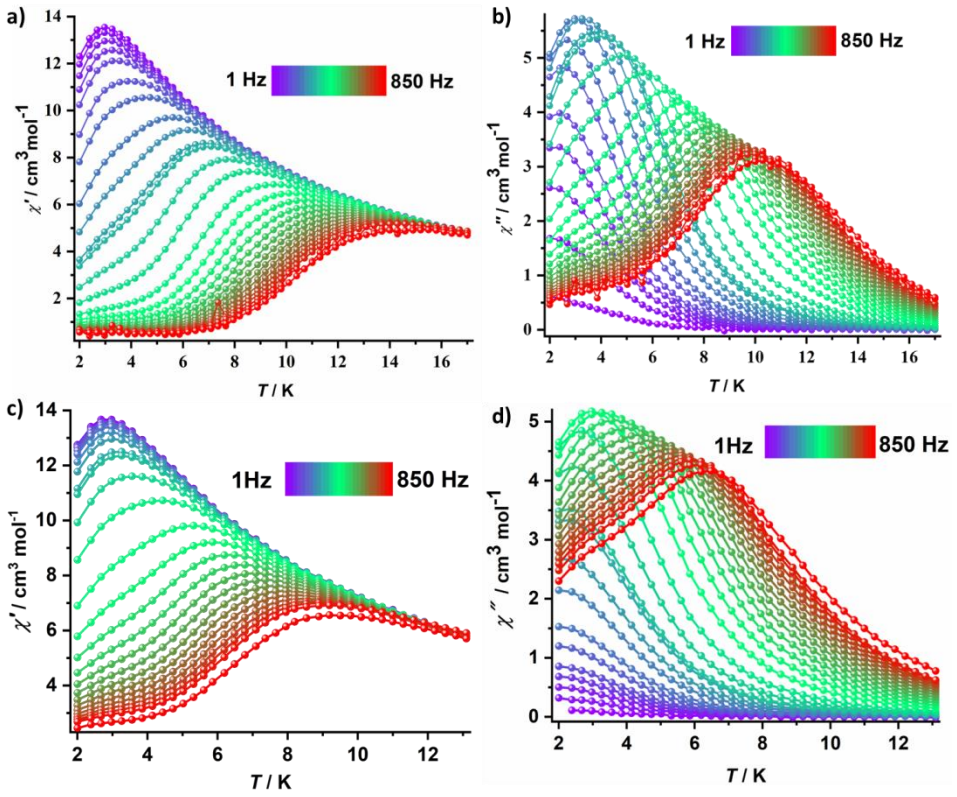

Figure S11. The in–phase (χ′) and out–of–phase (χ'') signals of the temperature dependence of ac susceptibility signals at given frequencies under absence of DC field for complexes **2**–**3** (a–d)

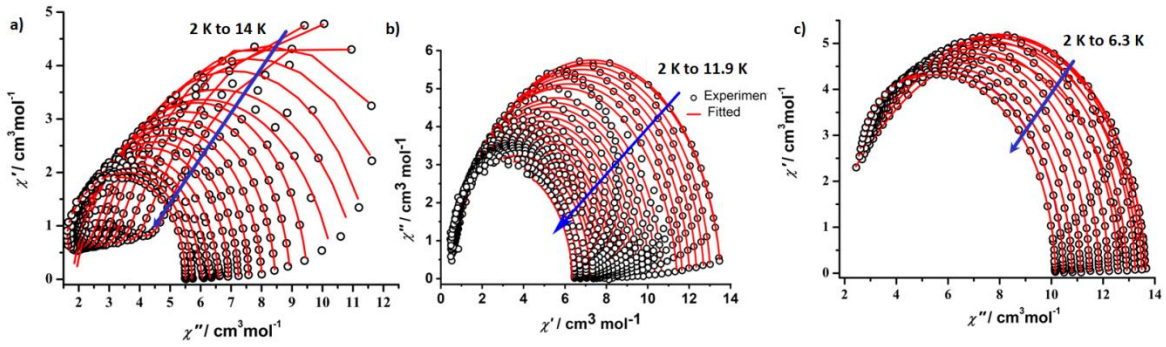

Figure S12. Cole Cole plot for complexes **1–3** (a–c) in a zero static field.

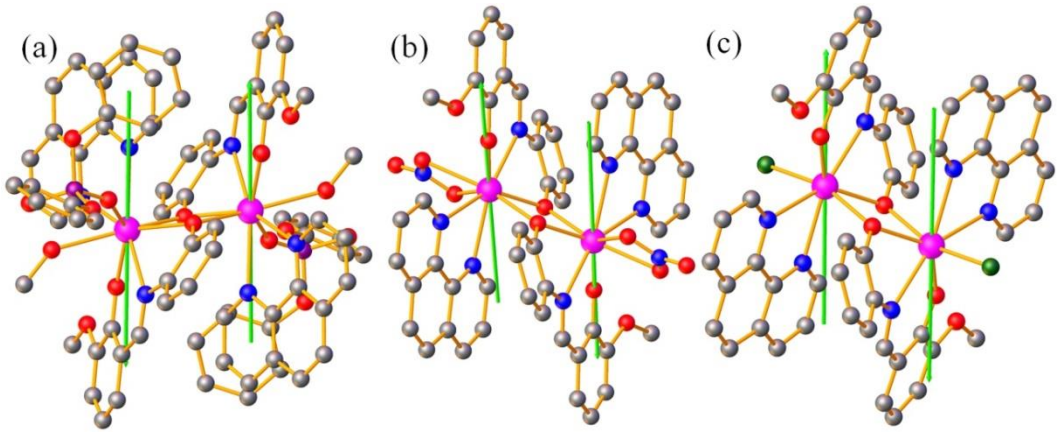

Figure S13. Single_Aniso computed local anisotropy axis g_z (green lines) for complexes **1-3** (a-c).

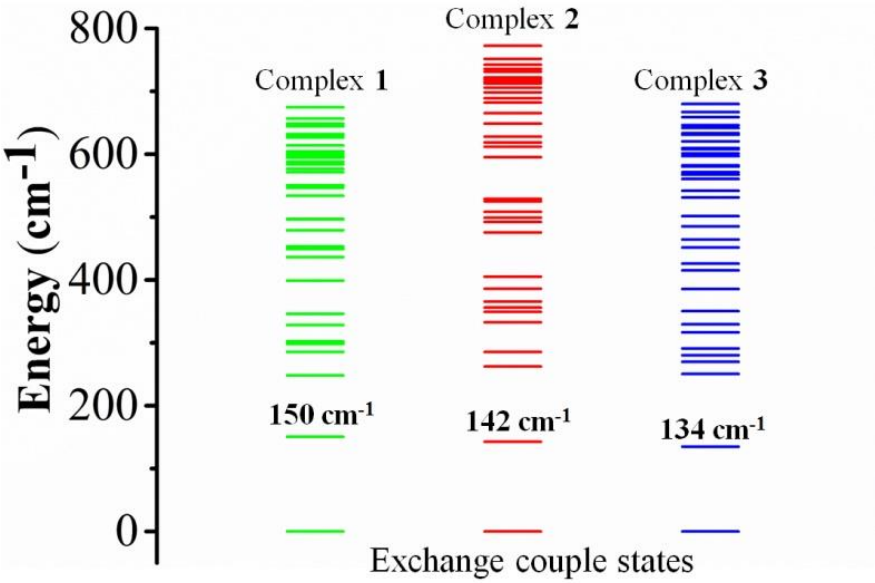

Figure S14: Energy of the exchange coupled state obtained from the simulation of susceptibility data using PHI for complexes **1-3**.

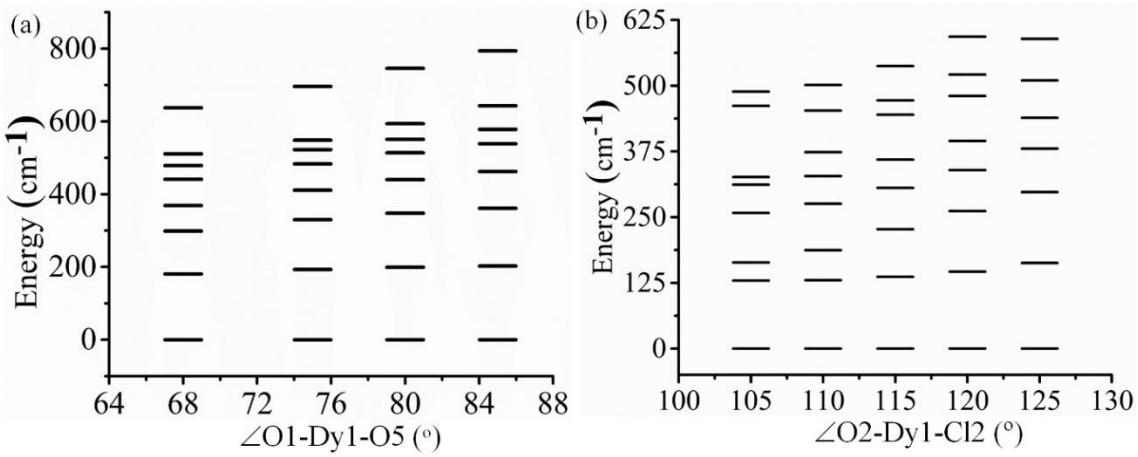

Figure S15: The energy of the KDs with the change of bond angle of the model complexes **1a-1d** (a) and **3-3d** (b).

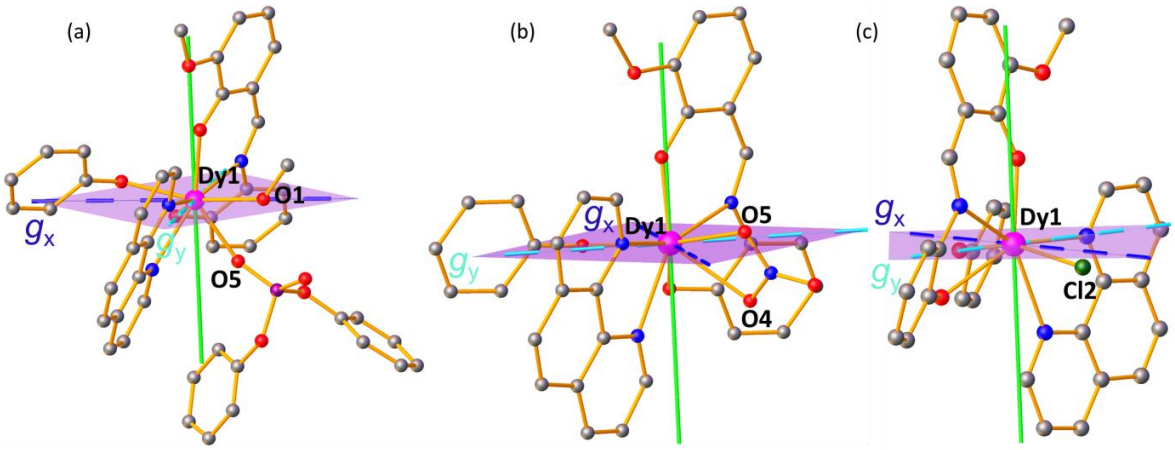

Figure S16: Represents the hard axes planes for complexes **1**(a), **2**(b) and **3** (c)

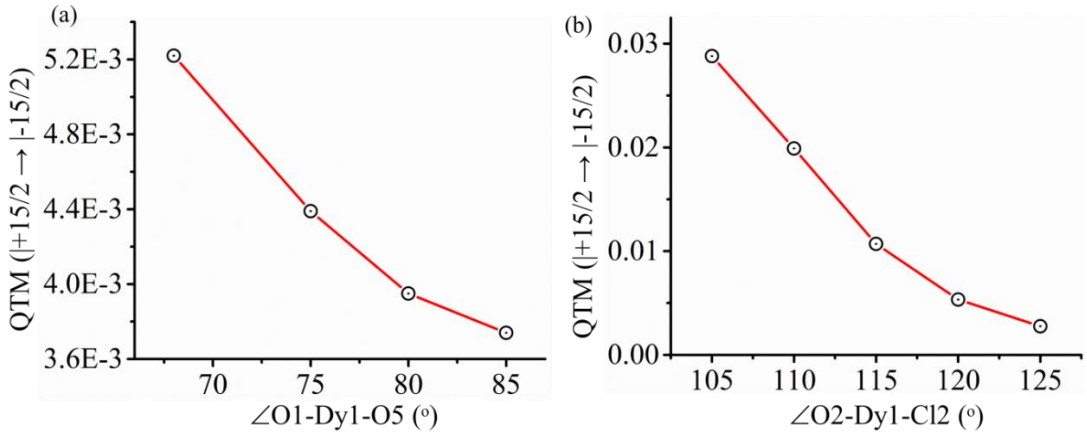

Figure S17: Change of QTM between the ground state KDs with the respective bond angle for model complexes **1a-1d** (a) and **3-3d** (b)

Table S1: X-ray crystallographic data

	Complex **1**	Complex **2**	Complex **3**
Formula	$C_{78}H_{66}Dy_2N_6O_{16}P_2$	$C_{52}H_{38}Dy_2N_8O_{12}$	$C_{52}H_{38}Cl_2Dy_2N_6O_6$
M_w (g mol^{-1})	1730.30	1291.90	1238.78
Crystal system	Monoclinic	Monoclinic	Monoclinic
Space group	$P2_1/n$	C2/c	$P2_1/n$
T (K)	140.0	140.0	140(2)
a (Å)	12.3944(10)	23.4456(15)	11.5978(3)
b (Å)	16.8447(14)	14.2211(8)	11.6814(3)
c (Å)	17.3271(14)	14.9699(8)	17.3607(4)
α (°)	90	90	90
ß(°)	103.003(2)	104.704(2)	95.2840(10)
γ(°)	90	90	90
V (Å^3)	3524.8(5)	4827.8(5)	2342.01(10)
Z	2	4	2
ρ_{calcd} (g cm^{-3})	1.630	1.777	1.757
μ(MoKα) (mm^{-1})	2.224	3.146	3.338
F(000)	1732.0	2536.0	1212.0
Collected reflections	59685	21543	15257
Independent reflections	7278	4594	4300
Goodness-of-fit (GOF) on F^2	1.027	1.070	0.920
R1, (I > 2σI[a]	0.0393	0.0537	0.0249
wR2, (I > 2σI)[a]	0.0591	0.1011	0.0487
CCDC Number	1987110	1987111	1987112

[a] $R_1 = \Sigma||F_o| - |F_c||/\Sigma|F_o|$ and $wR_2 = |\Sigma w(|F_o|^2 - |F_c|^2)|/\Sigma|w(F_o)^2|^{1/2}$

Table S2: Relevant bond distances (Å) for complexes **1–3**

1		2		3	
Dy1–Dy1[1]	3.8509(5)	Dy1–Dy1[1]	3.7510(7)	Dy1–Dy1[1]	3.7326(3)
Dy1– O2	2.350(3)	Dy1– O3[1]	2.305(5)	Dy1– Cl2	2.6172(9)
Dy1– O2[1]	2.317(3)	Dy1– O3	2.317(5)	Dy1– O3[1]	2.311(2)
Dy1– O3	2.201(3)	Dy1– O4	2.465(6)	Dy1– O3	2.313(2)
Dy1– O5	2.333(3)	Dy1– O2	2.156(6)	Dy1– O2	2.150(2)
Dy1– N3	2.542(3)	Dy1– O5	2.461(5)	Dy1– N3	2.464(3)
Dy1– O1	2.476(3)	Dy1– N1	2.548(6)	Dy1– N2	2.529(3)
Dy1– N1	2.476(3)	Dy1– N3	2.461(7)	Dy1– N1	2.515(3)
Dy1– N2	2.570(3)	Dy1– N2	2.507(6)		

Complex **1:** [1]1-X,1-Y,1-Z; Complex **2:** [1]1/2-X,3/2-Y,1-Z; Complex **3**: [1]-X,-Y,1-Z

Table S3. Relevant bond angles (°) around the metal centers found in complexes **1**–**3**

Complex 1

Atom	Atom	Atom	Angle/°	Atom	Atom	Atom	Angle/°
O2[1]	Dy1	Dy1[1]	34.67(6)	C27	C22	C23	119.8(4)
O2	Dy1	Dy1[1]	34.13(6)	C6	N2	Dy1	119.4(3)
O2[1]	Dy1	O2	68.80(10)	C2	N2	Dy1	123.2(3)
O2[1]	Dy1	O5	132.66(9)	C2	N2	C6	117.4(4)
O2	Dy1	N3	86.42(10)	C22	C23	N1	115.2(4)
O2[1]	Dy1	N3	76.18(10)	C24	C23	N1	124.9(4)
O2[1]	Dy1	O1	153.50(10)	C24	C23	C22	119.9(4)
O2	Dy1	O1	136.95(10)	N3	C7	C6	117.0(4)
O2[1]	Dy1	N1	107.68(10)	N3	C7	C11	122.7(4)

O2	Dy1	N1	66.41(10)	C11	C7	C6	120.3(4)
O2[1]	Dy1	N2	84.04(10)	C10	C9	C8	119.0(4)
O2	Dy1	N2	144.07(10)	O3	C15	C20	123.8(4)
O3	Dy1	Dy1[1]	103.46(7)	O3	C15	C16	118.8(4)
O3	Dy1	O2	119.13(10)	C20	C15	C16	117.4(4)
O3	Dy1	O2[1]	83.87(10)	C35	C34	O7	123.9(4)
O3	Dy1	O5	141.85(10)	C39	C34	O7	115.7(4)
O3	Dy1	N3	139.04(11)	C39	C34	C35	120.3(4)
O3	Dy1	O1	76.95(10)	N2	C6	C7	118.5(4)
O3	Dy1	N1	72.64(11)	N2	C6	C5	123.3(4)
O3	Dy1	N2	78.93(11)	C5	C6	C7	118.2(4)
O5	Dy1	Dy1[1]	104.58(7)	C15	C20	C21	121.7(4)
O5	Dy1	O2	75.18(9)	C15	C20	C19	119.7(4)
O5	Dy1	N3	71.83(10)	C19	C20	C21	118.4(4)
O5	Dy1	O1	70.99(10)	C22	C27	C26	119.4(4)
O5	Dy1	N1	83.81(10)	O4	C16	C15	113.7(4)
O5	Dy1	N2	110.82(10)	O4	C16	C17	125.2(4)
N3	Dy1	Dy1[1]	79.52(7)	C17	C16	C15	121.1(5)

[1]1-X,1-Y,1-Z

Complex 2

Atom	Atom	Atom	Angle/˚	Atom	Atom	Atom	Angle/˚
O3	Dy1	Dy11	35.64(12)	O5	N4	Dy1	58.1(4)
O31	Dy1	Dy11	35.85(13)	O5	N4	O4	116.3(6)
O31	Dy1	O3	71.5(2)	O6	N4	Dy1	178.2(6)
O31	Dy1	O4	141.3(2)	O6	N4	O4	121.6(8)
O3	Dy1	O4	79.76(18)	O6	N4	O5	122.1(8)
O3	Dy1	O5	128.56(19)	C8	N3	Dy1	128.7(7)
O31	Dy1	O5	159.0(2)	C8	N3	C9	121.9(8)
O31	Dy1	N1	77.32(19)	C9	N3	Dy1	109.4(5)
O3	Dy1	N1	80.1(2)	C25	N2	Dy1	118.8(5)
O3	Dy1	N4	104.3(2)	C24	N2	Dy1	122.9(5)
O31	Dy1	N4	162.5(2)	C24	N2	C25	117.8(7)
O3	Dy1	N3	67.3(2)	C26	C18	C19	118.1(9)
O31	Dy1	N3	111.40(19)	C17	C18	C26	117.9(8)
O31	Dy1	N2	82.01(19)	C17	C18	C19	124.1(8)
O3	Dy1	N2	140.2(2)	N1	C26	C18	122.0(8)
O4	Dy1	Dy11	111.69(14)	N1	C26	C25	117.8(7)
O4	Dy1	N1	72.6(2)	C18	C26	C25	120.2(8)
O4	Dy1	N4	26.0(2)	C16	C17	C18	120.1(8)

O4	Dy1	N2	106.1(2)	C17	C16	C15	118.7(9)
O2	Dy1	Dy11	110.24(15)	N1	C15	C16	123.4(9)
O2	Dy1	O31	88.8(2)	C20	C19	C18	122.2(9)
O2	Dy1	O3	125.5(2)	C11	C10	C9	118.7(10)
O2	Dy1	O4	129.5(2)	N3	C8	C4	126.6(9)
O2	Dy1	O5	83.3(2)	O3	C14	C13	121.9(8)
O2	Dy1	N1	145.5(2)	O3	C14	C9	117.7(8)
O2	Dy1	N4	106.7(2)	C13	C14	C9	120.3(8)
O2	Dy1	N3	74.5(3)	C25	C21	C20	117.9(9)
O2	Dy1	N2	81.7(2)	C22	C21	C25	117.2(8)
O5	Dy1	Dy11	163.43(16)	C22	C21	C20	124.8(8)
O5	Dy1	O4	51.9(2)	N2	C25	C26	118.6(7)
O5	Dy1	N1	98.4(2)	N2	C25	C21	121.7(8)
O5	Dy1	N4	25.9(2)	C21	C25	C26	119.7(8)
O5	Dy1	N3	85.3(2)	C19	C20	C21	121.9(9)
O5	Dy1	N2	77.6(2)	C12	C13	C14	120.0(9)

[1]1/2-X,3/2-Y,1-Z

Complex 3

Atom	Atom	Atom	Angle/°	Atom	Atom	Atom	Angle/°
Cl2	Dy1	Dy1[1]	136.51(2)	C12	C4	C5	118.6(4)
O3	Dy1	Dy1[1]	36.16(5)	C14	C19	N3	115.2(3)
O3[1]	Dy1	Dy1[1]	36.18(5)	C18	C19	C14	119.7(3)
O3[1]	Dy1	Cl2	162.01(6)	C18	C19	N3	125.1(3)
O3	Dy1	Cl2	102.73(6)	C12	N2	Dy1	118.8(2)
O3[1]	Dy1	O3	72.34(8)	C1	N2	Dy1	123.3(2)
O3[1]	Dy1	N3	107.85(8)	C1	N2	C12	117.9(3)
O3	Dy1	N3	67.55(8)	C2	C3	C4	119.8(4)
O3	Dy1	N2	80.24(8)	C3	C2	C1	118.9(4)
O3[1]	Dy1	N2	79.45(8)	C10	N1	Dy1	122.7(2)
O3	Dy1	N1	140.99(8)	C10	N1	C11	118.2(3)
O3[1]	Dy1	N1	83.13(8)	C11	N1	Dy1	118.8(2)
O2	Dy1	Dy1[1]	113.45(6)	C16	C17	C18	119.5(4)
O2	Dy1	Cl2	105.12(7)	N3	C20	C22	126.3(3)
O2	Dy1	O3[1]	90.78(8)	O2	C21	C26	118.5(3)
O2	Dy1	O3	128.95(8)	O2	C21	C22	123.6(3)
O2	Dy1	N3	73.14(9)	C22	C21	C26	117.9(3)
O2	Dy1	N2	144.87(9)	O1	C26	C21	113.3(3)
O2	Dy1	N1	79.93(9)	O1	C26	C25	126.0(3)
N3	Dy1	Dy1[1]	87.32(6)	C25	C26	C21	120.7(4)

N3	Dy1	Cl2	85.21(7)	C4	C12	C11	119.6(3)
N3	Dy1	N2	141.99(9)	N2	C12	C4	122.1(3)
N3	Dy1	N1	150.83(9)	N2	C12	C11	118.2(3)
N2	Dy1	Dy1[1]	77.39(6)	C17	C16	C15	121.2(3)
N2	Dy1	Cl2	82.67(6)	N1	C11	C12	118.3(3)
N1	Dy1	Dy1[1]	114.04(6)	N1	C11	C7	122.5(3)
N1	Dy1	Cl2	91.29(7)	C7	C11	C12	119.2(3)

[1]-X,-Y,1-Z

Table S4: Table for SHAPE calculations complex **1**–**2**

OP-8	1	D_{8h}	Octagon
HPY-8	2	C_{7v}	Heptagonal pyramid
HBPY-8	3	D_{6h}	Hexagonal bipyramid
CU-8	4	O_h	Cube
SAPR-8	5	D_{4d}	Square antiprism
TDD-8	6	D_{2d}	Triangular dodecahedron
JGBF-8	7	D_{2d}	Johnson gyrobifastigium J26
JETBPY-8	8	D_{3h}	Johnson elongated triangular bipyramid J14
JBTPR-8	9	C_{2v}	Biaugmentedtrigonal prism J50
BTPR-8	10	C_{2v}	Biaugmentedtrigonal prism
JSD-8	11	D_{2d}	Snub diphenoid J84
TT-8	12	T_d	Triakis tetrahedron
ETBPY-8	13	D_{3h}	Elongated trigonalbipyramid

[ML_8]	OPY-8	HPY-8	HBPY-8	CU-8	**SAPR-8**	TDD-8	JGBF-8	JETBPY-8	JBTPR-8	BTPR-8	JSD-8	TT-8	ETBPY-8
Dy1 (complex **1**)	32.432	19.898	13.804	8.752	**1.219**	2.532	14.745	27.549	3.694	2.554	6.010	9.513	23.854

Dy1 (complex **2**)	33.469	20.809	16.481	10.972	**1.740**	2.575	15.475	27.014	3.661	3.017	5.844	11.686	22.186

Table S5: Table for SHAPE calculations for complex **3**

HP-7	1	D7h	Heptagon
HPY-7	2	C6v	Hexagonal pyramid
PBPY-7	3	D5h	Pentagonal bipyramid
COC-7	4	C3v	Capped octahedron
CTPR-7	5	C2v	Capped trigonal prism
JPBPY-7	6	D5h	Johnson pentagonal bipyramid J13
JETPY-7	7	C3v	Johnson elongated triangular pyramid J7

[ML_7]	HP-7	HPY-7	PBPY-7	COC-7	CTPR-7	JPBPY-7	JETPY-7
Dy1 (complex **3**)	31.475	21.608	**2.762**	3.408	3.345	6.767	17.461

BS-DFT Calculations

To gain insight into the magnetic exchange coupling between the Dy centers in both the compounds we performed density functional theory (DFT) calculations in combination with broken symmetry (BS) approach to obtain information on exchange couplings within the ORCA 4.0 software package.[1] Also the relativistic effects were included with the zero order regular approximation (ZORA), together with the scalar relativistic contracted version of the basis functions def2-TZVP for Gd, and def2-TZVP(-f) for Cl, P, N, O, C and H atoms. In these calculations the well-known B3LYP functional was employed to extract the isotropic exchange couplingusing the method of Yamaguchi where the exchange coupling is determined from the energies (E) and expectation values ($<S^2>$) of the triplet and broken symmetry singlet states. Later the obtained isotropic exchange coupling constant *J* has been rescaled to the pseudo spin ½ of the corresponding lanthanide atoms.

$$J = \frac{-(E_T - E_{BSS})}{\langle S^2 \rangle_T - \langle S^2 \rangle_{BSS}} \quad \text{.....Eq. x}$$

Table S6: Energy of the high spin and broken symmetry state

Energy of the high spin and broken symmetry state for 1		
Spin State	Energy (Hatree)	$<S^2>$
HS	-26213.457291	57.0109
BS	-26213.457026	8.0096
Energy of the high spin and broken symmetry state for 2		
HS	-26392.439506	56.0127
BS	-26392.439539	7.0127
Energy of the high spin and broken symmetry state for 3		
HS	-26755.988898	56.0133
BS	-26755.988933	7.0133

Table S7. Fitting and BS-DFT calculated parameters for complexes1-3.

Used parameters for fitting	**Complex 1**	**Complex 2**	**Complex 3**
J (cm^{-1})	-0.073	-0.103	-0.078
g	1.3	1.3	1.3
zJ' (cm^{-1})	-0.008	+0.0016	-0.0131
B_0^2	-0.1748E+01	-0.2155E+01	-0.1758E+01
B_0^4	-0.4417E-02	-0.4897E-02	-0.5583E-02
B_0^6	0.6357E-05	0.1297E-04	0.1880E-04
B_6^6	0.2125E-03	-0.1336E-03	0.1357E-03
BS-DFT calculated J (cm^{-1})	+2.33	-0.294	-0.313

Table S8: Relaxation barriers for selected Dy2-SMMs under a zero *dc* field

	Complex	Geometry	Donor ; CN	magnetic interaction	Ueff (K)	Reference
1	$[Dy_2(nb)_4(H_2L)_2]$	biaugmented trigonal prism	NO_7; 8	AF	277.7	7a
3	$[Dy_2(HL_1)_2Cl_2(H_2O)_3]\cdot 2H_2O\cdot MeCN$	hula-hoop; pentagonal bipyramidal	N_2O_6; 8; $N_2O_3Cl_2$; 7	F	204; 103	9e
4	$[Dy_2(valdien)_2(NO_3)_2]$	dodecahedral	N_3O_5, 8	AF	76	9g
5	$[Dy_2(Mq)_4Cl_6](EtOH)_2$	octahedral	O3Cl3 , 6	AF	102.4	18a
6	$[Dy_2(Py_3CO)_2(PhCOO)_4(MeOH)_2]\cdot MeOH$	hula-hoop	N3O5, 8	F	51 K	18b
7	$[Dy_2(MeOH)_2(HL^1)_2(NO_3)_2]\cdot 2MeOH$	—	NO7	F	34 K	18c
8	$[Dy_2(ovph)_2Cl_2(MeOH)_3]\bullet MeCN$	hula-hoop; pentagonal bipyramidal	N_2O_6, 8; $N_2O_3Cl_2$,7	F	150; 198	18d
9	$[Dy_2(CH_3OH)_2(HL_2)_2(PhCOO)_2]$	dodecahedral	NO_7, 8	F	94	18e
10	$[Dy_2(H_2O)_2(ovph)_2(NO_3)_2]$	dodecahedral	N_2O_6, 8	F	69	18f
11	$[Dy_2(TTA)_2(L)_2(CH_3OH)_2]2CH_2Cl_2$	biaugmented trigonal prism	N_2O_6, 8	F	102	18g
12	$[Dy_2(tfa)_2(L)_2(CH_3OH)_2]$	biaugmented trigonal prism	N_2O_6, 8	F	140	18g
13	$[Dy_2(a'povh)_2(OAc)_2(DMF)_2]$	dodecahedral	N_2O_6; 8	AF	322.1	24
14	$\{Dy_2\ (L_1)_2\ (L_2)_2$ (diphenyl phosphate)$_2(MeOH)_2\}$	square antiprism	N_3O_5	AF	229.41 (159.45 cm^{-1})	This work
15	$\{Dy_2\ (L_1)_2\ (L_2)_2\ (NO_3)_2\}$	square antiprism	N_3O_5	AF	90.09 (62.62 cm^{-1})	This work

Table S9: Single_Anios calculated crystal field parameter for complexes **1**-**3**.

k	Q	Complex 1	Complex 2	Complex 3
2	-2	-0.1241E+00	0.1186E+00	0.1384E+00
	-1	-0.2483E+00	0.2372E+00	0.2768E+00
	0	-0.1748E+01	-0.2155E+01	-0.1758E+01
	1	0.1476E+01	-0.1731E+01	-0.1403E+01
	2	-0.1368E+00	-0.3070E+00	-0.9980E+00
4	-4	0.5838E-02	0.1764E-01	0.6116E-02
	-3	0.1651E-01	0.4989E-01	0.1729E-01
	-2	0.4413E-02	0.1333E-01	0.4623E-02
	-1	0.6241E-02	0.1885E-01	0.6538E-02
	0	-0.4417E-02	-0.4897E-02	-0.5583E-02
	1	0.1650E-02	-0.1755E-02	0.1188E-01
	2	-0.5190E-02	0.3806E-02	0.1691E-01
	3	-0.1016E+00	0.1049E-01	0.5209E-01
	4	-0.1329E-01	0.2420E-01	-0.3988E-01
6	-6	-0.3117E-04	-0.9273E-04	-0.8716E-04
	-5	-0.1079E-03	-0.3212E-03	-0.3019E-03
	-4	-0.2302E-04	-0.6848E-04	-0.6437E-04
	-3	-0.4203E-04	-0.1250E-03	-0.1175E-03
	-2	-0.2101E-04	-0.6252E-04	-0.5876E-04
	-1	-0.2658E-04	-0.7908E-04	-0.7433E-04
	0	0.6357E-05	0.1297E-04	0.1880E-04
	1	-0.1002E-03	0.2300E-03	-0.5919E-04
	2	0.1204E-03	-0.1176E-04	0.4003E-04
	3	-0.6663E-04	0.3021E-04	-0.1581E-04
	4	-0.1454E-03	0.1717E-03	-0.5644E-04
	5	-0.7519E-04	-0.8581E-03	0.9992E-03
	6	0.2125E-03	-0.1336E-03	0.1357E-03

Table S10: Single_aniso computed energy of the KDs, g and wavefuctions composition for complex **1**.

Kramers doublets	Energy (cm^{-1})	g_x	g_y	g_z	angle (°)	Wavefunction composition
1	0.000	0.0001	0.0097	19.76		97.92%|±15/2>+1.52%|±9/2>
2	124.528	0.459	0.793	15.784	8.83	81.18%|±13/2>+6%|±7/2>+4.2%|±9/2>+3.33%|±5/2>+2.1%|±3/2>+1.7%|±1/2>
3	186.321	2.915	3.442	11.277	28.59	50%|±11/2>+12.5%|±5/2>+10%|±3/2>+9%|±7/2>+8.2%|±1/2>+6.1%|±13/2>+5%|±9/2>
4	246.541	7.440	6.624	1.718	102.85	38%|±9/2>+15%|±3/2>+20.2%|±11/2>+10.4%|±1/2>+8.8%|±7/2>+3.2%|±5/2>
5	284.716	1.815	5.598	10.613	81.78	36%|±1/2>19%|±5/2>+18.3%|±7/2>+13.6%|±9/2>+8%|±3/2>+4.8%|±11/2>
6	311.207	0.560	1.653	15.940	85.93	33%|±3/2>+25%|±5/2>+18.6%|±7/2>+14.7%|±1/2>+5.8%|±9/2>+2.7%|±11/2>
7	399.893	0.046	0.066	19.781	78.20	26.6%|±1/2>+25%|±3/2>+20.9%|±5/2>+16.2%|±7/2>+7.8%|±9/2>+2.9%|±11/2>
8	525.312	0.009	0.029	19.886	59.13	24.7%|±9/2>+23.1%|±7/2>+17.1%|±11/2>+16.3%|±5/2>+8%|±3/2>+6.4%|±13/2>+3.7%|±1/2>

Table S11: Single_aniso computed energy of the KDs, g and wavefuctions composition for complex **2**.

Kramers doublets	Energy (cm^{-1})	g_x	g_y	g_z	angle (°)	Wavefunction composition
1	0.000	0.036	0.039	19.844		99.02%|±15/2>+0.62%|±7/2>
2	141.726	0.357	0.478	17.002	164.73	85.84%|±13/2>+9.35%|±11/2>+2.48%|±5/2>+1.13%|±7/2>
3	235.773	4.190	4.764	11.377	146.14	42.41%|±11/2>+20.5%|±9/2>+11.85%|±5/2>+9.9%|±3/2>+6.3%|±7/2>+6%|±13/2>+3%|±1/2>
4	280.349	1.042	5.058	12.116	93.57	30%|±3/2>+20.08%|±1/2>+15.22%|±9/2>+14%|±11/2>+12%|±5/2>+5.6%|±7/2>
5	306.723	0.551	3.505	11.033	102.85	37.5%|±1/2>26.3%|±7/2>+15%|±9/2>+10%|±11/2>+6.2%|±5/2>+3.6%|±3/2>+1.5%|±13/2>
6	383.889	0.937	2.658	15.474	99.29	25.6%|±5/2>+22%|±3/2>+21.6%|±7/2>+14.8%|±9/2>+5.8%|±9/2>+6.5%|

						±1/2>+7.2%|±11/2>+2.24%|±13/2>
7	453.055	0.802	1.101	18.341	71.70	18%|±3/2>+22.5%|±5/2>+15.2%|±7/2>+15%|±9/2>+17.4%|±1/2>+9.8%|±11/2>+2 %|±13/2>
8	585.882	0.067	0.194	19.560	67.33	13%|±1/2>+16.34%|±3/2>+19.2%|±5/2>+23.54%|±7/2>+19.25%|±9/2>+7.3%|±11/2>+1.2%|±13/2>

Table S13: Single_aniso computed energy of the KDs, g and wavefuctions composition for complex **3**.

Kramers doublets	Energy (cm^{-1})	g_x	g_y	g_z	angle (°)	Wavefunction composition
1	0.000	0.075	0.096	19.775		97.31%|±15/2>+1.70%|±11/2>
2	129.341	1.263	5.728	12.539	26.63	62%|±13/2>+5%|±7/2>+7%|±5/2>+23.74%|±3/2>+11%|±1/2>
3	163.639	2.914	3.642	11.006	71.18	30%|±13/2>+6%|±11/2>+7%|±9/2>+3%|±7/2>+11%|±5/2>+13%|±3/2>+30%|±1/2>
4	257.829	4.543	6.541	8.973	14.98	60%|±11/2>+16%|±3/2>+10%|±1/2>+5%|±9/2>+2.2%|±5/2>+4%|±7/2>
5	311.823	1.022	2.240	10.181	77.42	8%|±11/2>19%|±9/2>+21%|±7/2>+32%|±5/2>+9%|±3/2>+12%|±1/2>
6	326.109	1.024	3.938	12.237	56.83	37%|±9/2>+25%|±7/2>+12%|±11/2>+7%|±5/2>+4%|±1/2>
7	461.476	0.991	2.989	15.491	74.51	21%|±5/2>+17%|±9/2>+13%|±7/2>+19%|±3/2>+22%|±1/2>+9%|±11/2>
8	488.610	0.622	3.786	16.384	108.78	31%|±7/2>+17%|±9/2>+22%|±5/2>+17%|±3/2>+12%|±1/2>+4%|±11/2>

Computational Methods:

The *ab initio* calculations were performed with MOLCAS 8.2 software package. For all the atoms ANO-RCC basis set of function were used as [ANO-RCC...6s5p3d1f.] for Dy, [ANO-RCC...6s5p3d1f.] for Lu, [ANO-RCC...4s3p1d.] for P, [ANO-RCC...3s2p1d.] for O and N, [ANO-RCC...3s2p.] for C and [ANO-RCC...2s.] for H, including the relativistic effects within Douglas Kroll Hess Hamiltonian.[2] To save the disk space the Cholesky decomposition for two electrons integral was employed throughout the calculations. We have included nine electrons in seven metal based 'f' orbitals, CAS (9, 7) in the active space of CASSCF calculations and 21 sextets in the RASSCF method. The RASSI-SO program[3] has been used to include the spin orbit coupling in the 21 sextets optimized in the previous calculations. The SINGLE_ANISO module[4] was used to calculate the energy, the transition matrix element between the KDs and relevant information.

References:

1. F. Neese, The ORCA program system, *WIREs Comput. Mol. Sci.*, 2012, **2**, 73-78.

2. (a) Douglas, M.; Kroll, N. M. Quantum electrodynamical corrections to the fine structure of helium. *Ann. Phys.* **1974,** *82*, 89-155. (b) Hess, B. A., Relativistic electronic-structure calculations employing a two-component no-pair formalism with external-field projection operators. *Phys. Rev. A* **1986,** *33*, 3742-3748. (c) Reiher, M. Relativistic Douglas–Kroll–Hess theory. *WIREs Comput. Mol. Sci.* 2012, 2, 139-149.

3. Malmqvist, P. Å.; Roos, B. O.; Schimmelpfennig, B. The restricted active space (RAS) state interaction approach with spin–orbit coupling. *Chem. Phys. Lett.* **2002,** *357*, 230-240.

4. Chibotaru, L. F.; Ungur, L. Ab initio calculation of anisotropic magnetic properties of complexes. I. Unique definition of pseudospin Hamiltonians and their derivation. *J. Chem. Phys.* ***2012,*** *137*, 064112.